High-Q Nanomechanics via Destructive Interference of Elastic Waves

I. Wilson-Rae, R. A. Barton, S. S. Verbridge, D. R. Southworth, B. Ilic, H. G. Craighead, and J. M. Parpia

High-Q Nanomechanics via Destructive Interference of Elastic Waves

I. Wilson-Rae,[1, *] R.A. Barton,[2] S.S. Verbridge,[2] D.R. Southworth,[2] B. Ilic,[2] H.G. Craighead,[2] and J.M. Parpia[2]

[1] *Technische Universität München, 85748 Garching, Germany.*
[2] *Center for Materials Research, Cornell University, Ithaca, NY, 14853 USA*

Mechanical dissipation poses an ubiquitous challenge to the performance of nanomechanical devices. Here we analyze the support-induced dissipation of high-stress nanomechanical resonators. We develop a model for this loss mechanism and test it on Si_3N_4 membranes with circular and square geometries. The measured Q-values of different harmonics present a non-monotonic behavior which is successfully explained. For azimuthal harmonics of the circular geometry we predict that destructive interference of the radiated waves leads to an exponential suppression of the clamping loss in the harmonic index. Our model can also be applied to graphene drums under high tension.

Nanomechanical resonators offer great potential for practical device applications that exploit their ultra-low mass and high frequencies [1]. Examples range from scaling scanning-probe force microscopy and mass-sensing down to the molecular scale to providing alternatives for radio frequency devices. In turn, measurements of mechanical displacements with an imprecision below the standard quantum limit and the preparation of ultracold motional states have already been implemented with electromechanical [2–4] and optomechanical systems [5, 6]. These breakthroughs foreshadow the possibility of realizing a "quantum optics" analogue involving a macroscopic mechanical degree of freedom which would set a new stage for fundamental tests and potential quantum devices [4, 7, 8]. All of these endeavors share the desirability of minimizing the mechanical dissipation which can be quantified, for example, in terms of the damping coefficient $\Gamma = m_R\omega_R/Q$ — where m_R is the resonator's effective mass, ω_R its resonant angular frequency and Q its quality-factor (Q-value). In fact, though the figures of merit for these various applications are quite diverse, in all instances performance is enhanced if Q is increased while m_R and ω_R are kept approximately constant [1, 8, 9]. Finally, with the advent of the use of stressed silicon nitride membranes, nanomechanical devices with remarkably low dissipation ($\Gamma \sim 10^{-14}\,\mathrm{Kg\,s^{-1}}$ and $Q \sim 10^6$) have already been demonstrated [9–15].

In this letter, we present and test a model that captures the energy loss that occurs due to elastic wave radiation [16–20] at the periphery of these high-stress resonators. We show that this mechanism is significant in state of the art structures and is strongly influenced by interference effects. We compare the results of our model to measurements of the resonant modes of two configurations, a single "drum resonator" and a composite array of drum resonators that effectively realizes a square membrane [cf. Fig. 1 (a) and (b)]. We examine the harmonics of these structures and accurately account for much of the variation in the corresponding Q-values. Our analysis reveals that certain types of modes are inherently resilient to clamping loss as a result of destructive interference of the radiated waves. Thus, we provide insight into resonators that might be realized and yield better Q-values in the future. On general grounds, the fact that the relevant stress at the resonator-support contact scales at least linearly with frequency combined with the 3D nature of the support, lead to the naive expectation that the dissipation ($1/Q$) due to elastic-wave radiation should increase as one considers higher harmonics [cf. Eq. (1)]. In dramatic contrast, we find that for the harmonics of a circular membrane the clamping loss is exponentially suppressed as the number of radial nodal lines increases.

To derive an adequate model for the clamping losses, we adopt the phonon tunneling approach introduced in Ref. 17 and start from the general weak coupling expression for the dissipation $1/Q$ in terms of the "overlaps" between the resonator mode and the free modes of the substrate ("support"):

$$\frac{1}{Q} = \frac{\pi}{2\rho_s\rho_R\omega_R^3}\int_q\left|\int_S \mathrm{d}\bar{S}\cdot\left(\boldsymbol{\sigma}_q^{(0)}\cdot\bar{u}_R' - \boldsymbol{\sigma}_R'\cdot\bar{u}_q^{(0)}\right)\right|^2 \times \delta[\omega_R - \omega(q)]. \tag{1}$$

Here $\boldsymbol{\sigma}_R'$ and $\bar{u}_R'$ are the stress and displacement fields associated with the normalized resonator mode, $\boldsymbol{\sigma}_q^{(0)}$ and $\bar{u}_q^{(0)}$ are the analogous fields for the continuum of support free modes labeled by q [eigenfrequencies $\omega(q)$], and ρ_s and ρ_R are, respectively, the densities of the substrate and resonator materials. In our setting the resonator mode should satisfy clamped boundary conditions at the resonator-support contact area S while the unperturbed support modes should satisfy free boundary conditions implying that only the second term in Eq. (1) contributes. The substrate is modelled as a half-space that contacts the membrane resonator at its rim S — i.e. the under-etched gap between the suspended structure and the substrate is neglected when determining the support free modes (for our structures this gap was $\lesssim 200\mathrm{nm} \ll D$). We assume the "high stress" regime $\mathrm{t}^2/D^2 \ll \sigma/E_R \ll 1$, where σ is the tensile stress in the membrane, t its thickness, D its large dimension (diameter or side) and E_R the Young modulus of the resonator material. This implies
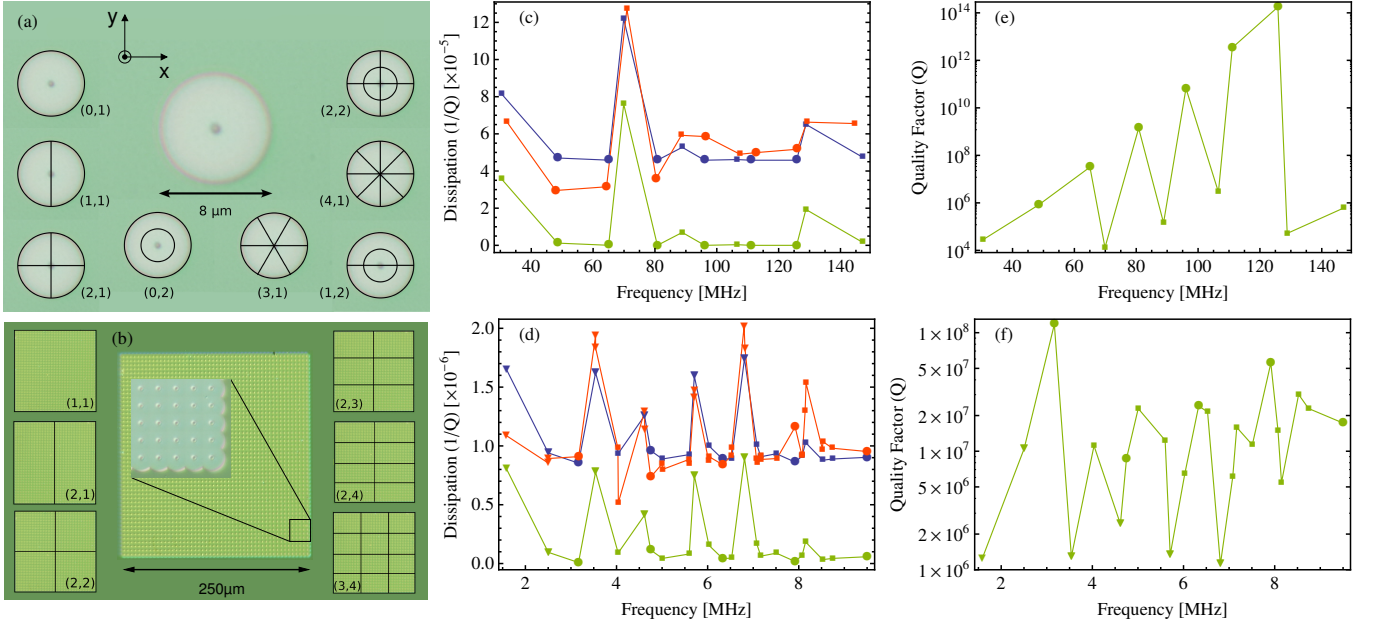
FIG. 1. (a) Micrograph of a single drum resonator (similar to the one used in our analysis) superposed with schematic diagrams of the different harmonics (n, m) depicting their nodal lines (the origin is set at the center of the membrane). (b) Idem for a square membrane resonator. (c) Dissipation $1/Q$ as a function of frequency for the different harmonics of a Si_3N_4 drum resonator ($D = 14.5\,\mu m$, $\mathsf{t} = 110$nm, and $\sigma = 0.90$ GPa). (d) Idem for a square membrane resonator ($253.2\,\mu m \times 253.2\,\mu m \times 0.0125\,\mu m$ with $\sigma = 0.87$ GPa). Red plot: Measured values with an error of 10% for $1/Q$ — we ascribe the splitting of degeneracies observed for the square membrane [cf. (d)] to disorder. Blue plot: Least squares fit of our model to the measured $1/Q$ using as fit parameters an internal dissipation offset ($1/Q_{int}$) and material properties of the substrate ($E_s = 148$ GPa, $\rho_s = 3.75$ gcm^{-3}, and $1/Q_{int} = 8.5 \times 10^{-7}$ for the square membrane, and $E_s = 323$ GPa, $1/Q_{int} = 4.6 \times 10^{-5}$ for the drum). Green plot: $1/Q$ without the offset corresponding to the predicted clamping loss — the resulting limits for the Q-values of the drum and square membrane are shown, respectively, in (e) and (f). High-Q harmonics $(n,1)|_{n>0}$ $[(n,n)|_{n>1}]$ of the drum [square] are marked by circles; low-Q harmonics $(n,1)|_{n>0}$ of the square, by triangles. For the drum [square] all harmonics with frequencies below 130 MHz [9 MHz] are included except $(0,3)$, $(3,2)$ $[(7,1)]$.

that bending effects are negligible and one can use the classical wave equation adequate for a taut membrane [21]. Thus for the drum's eigenfrequencies we obtain [cf. Fig. 1 (a), (b)]: $\omega_{nm} = 2\zeta_{nm}c_R/D$ with $n = 0, 1, \ldots$ and $m = 1, 2, \ldots$; while the square's eigenfrequencies are given by: $\omega_{nm} = \pi\sqrt{n^2 + m^2}\,c_R/D$ with $n, m > 0$ Here $c_R = \sqrt{\sigma/\rho_R}$ is the phase velocity in the membrane, and ζ_{nm} is the mth zero of the Bessel function $J_n(x)$. In this context, the weak coupling approximation underpinning Eq. (1) reads $\omega_{nm}\mathsf{t}/c_R \ll 1$ and the stress $\boldsymbol{\sigma}'_R$ corresponds to the variation with respect to equilibrium.

For the single drum we adopt support eigenmodes $\bar{u}^{(0)}_{q,\theta,l,\gamma}(\bar{r})$ (with $l = 0, \pm 1, \ldots$) that have axial symmetry with respect to z [cf. Fig. 1 (a)]. These are related to the plane wave eigenmodes $\bar{u}^{(0)}_{\bar{q},\gamma}(\bar{r})$ by: $\bar{u}^{(0)}_{q,\theta,l,\gamma}(\bar{r}) = [(-i)^n/\sqrt{2\pi}] \int_{-\pi}^{\pi} d\varphi\, e^{in\varphi} \bar{u}^{(0)}_{\bar{q},\gamma}(\bar{r})$; where $\gamma = l, t, s$ labels the different types of relevant modes [i.e. longitudinal (l), transverse SV (t), and SAW (s) given that SH waves do not contribute] with velocities of propagation c_γ, and we use spherical coordinates for the incident wavevector $\bar{q}(q, \theta, \varphi) = q(\sin\theta\cos\varphi, \sin\theta\sin\varphi, \cos\theta)$ [$\theta = \pi/2$ for $\gamma = s$ and $\theta \leq \pi/2$ otherwise]. Thus, substitution of the

support and resonator modes ($\omega_R \to \omega_{nm}$) into Eq. (1) (cf. [22]) leads to

$$\frac{1}{Q_{nm}} = \frac{4\pi^2 \zeta_{nm}\rho_R\mathsf{t}}{\rho_s D} \sum_{\gamma} \eta_\gamma^3 \tilde{u}_{n,\gamma}(\eta_\gamma\zeta_{nm}, \nu_s). \quad (2)$$

Here we introduce the dimensionless functions $\tilde{u}_{l,\gamma\neq s}(\tilde{q}, \nu_s) = 2\pi\int_0^{\pi/2} d\theta\sin\theta |u^{(0)}_{\bar{q},\gamma;z}(0, \nu_s)|^2 J_l^2(\tilde{q}\sin\theta)$, $\tilde{u}_{l,s}(\tilde{q}, \nu_s) = 2\pi|u^{(0)}_{\bar{q},s;z}(0, \nu_s)|^2 J_l^2(\tilde{q})$ and define $\eta_\gamma \equiv c_R/c_\gamma \sim \sqrt{\sigma\rho_s/E_s\rho_R}$ — where the prefactors of order unity, which depend on γ, are functions of the Poisson ratio for the substrate ν_s. We note that $|u^{(0)}_{\bar{q},\gamma;z}(0, \nu_s)|^2$ solely depends on γ, $\cos\theta$ and ν_s (cf. [22]).

In turn, for the square membrane an analogous procedure detailed in the [22], leads to:

$$\frac{1}{Q_{nm}} = \frac{16\pi n^2 m^2 \rho_R \mathsf{t}}{\sqrt{n^2 + m^2}\rho_s D} \sum_{l,\gamma} \eta_\gamma^3 \tilde{w}_{l,\gamma}^{n,m}(\sqrt{n^2 + m^2}\,\eta_\gamma, \nu_s)$$

$$(3)$$

with $\tilde{w}^{n,m}_{l,s}(\tilde{q}, \nu_s) = |u^{(0)}_{\bar{q},s;z}(0, \nu_s)|^2 \tilde{f}_{nml}(\tilde{q})$, $\tilde{w}^{n,m}_{l,\gamma\neq s}(\tilde{q}, \nu_s) = \int_0^{\pi/2} d\theta\sin\theta |u^{(0)}_{\bar{q},\gamma;z}(0, \nu_s)|^2 \tilde{f}_{nml}(\tilde{q}\sin\theta)$, where $l \geq 0$ and

we introduce $\tilde{f}_{nml}(x) = f_l(\pi x)[Z_{nml}(x) + Z_{mnl}(x)]$ with

$$Z_{nml}(x) \equiv \frac{z_{n<}^l(x)}{n^3 (n^2 - x^2)^{3/2}} \left\{ 2n(l+1)\sqrt{n^2 - x^2} + z_{n<}(x) \right.$$

$$\left. + \frac{16 n^2 (n^2 - x^2) z_{n<}(x)}{[z_{n<}(x) + z_{m>}(x)][z_{n<}(x) + z_{m<}(x)]} \right\}.$$

Here $z_{n\lessgtr}(x) \equiv 2n^2 - x^2 \mp 2n\sqrt{n^2 - x^2}$ and the functions $f_l(x)$ are given by: $f_l(x) \equiv [\delta_{0l} - 2(-1)^n J_{4l}(x) + (-1)^l J_{4l}(\sqrt{2}x)]/(2^{\delta_{0l}} x^{4l})$ for $n + m$ even, and $f_l(x) = [\delta_{0l} - 2\sin^2(l\pi/2) J_{2l}(x) - \cos(l\pi/2) J_{2l}(\sqrt{2}x)]/(2^{\delta_{0l}} x^{2l})$ for $n + m$ odd. Equation (3) is only valid for the case $\min\{n,m\} > \eta_s\sqrt{n^2 + m^2}$ which is satisfied for the resonances studied here — note that material properties always imply $\eta_l < \eta_t < \eta_s$, and $\sigma \ll E_s$ implies $\eta_s \ll 1$.

We proceed to compare the predictions of our model [Eqs. (2)-(3)] with the dissipation measured in nanomechanical membrane resonators (cf. Fig. 1). These resonators are made of "stoichiometric" Si_3N_4 deposited by low pressure chemical vapor deposition on SiO_2 [14]. The nitride has an inherent stress of $1.2\,GPa$, as measured by a wafer bow technique [10], and a density $\rho_R = 2.7\,gcm^{-3}$. After lithographic patterning to define access holes, the resonators are suspended by etching the underlying oxide through these holes, using buffered oxide etch (BOE) for the single drum and HF for the square membrane, and critical point dried. Thus a single access hole results in a circular drum geometry, while a square geometry is defined by a periodic square lattice of such holes (50×50 separated by $5\,\mu m$). Given the small size of the holes ($\lesssim 1\,\mu m$) compared with the typical mode wavelength, we neglect them in our model. For the square array, the same consideration applies to the hole separation so that we use a square membrane model with uniform thickness $t = 12.5\,nm$ given by the average over the array [23] and side $D = \sqrt{A} = 253.2\,\mu m$, where A is the suspended area. For the single drum (diameter $D = 14.5\,\mu m$) the use of a BOE etch implies that the thickness is uniform and equal to the nitride thickness (110nm).

The mechanical resonances of the structures are characterized under vacuum and room temperature conditions, using a technique described in Ref. 14. The resonators are actuated using a piezo disc that vibrates the chip in the out-of-plane direction and the motion is detected via a 633nm CW laser. Figure 1 (c)-(f) compares the measured frequencies and Q-values of different harmonics for the two configurations, single drum and square array, with the predictions of our model. This comparison takes into account three issues: (i) the release of the resonator leads to a local deformation of the wafer that lowers the membrane's tensile stress with respect to the one in the nitride layer, (ii) in addition to clamping losses the resonator will be affected by internal dissipation [11, 14, 15, 24, 25], and (iii) the parameters for the half-space model of the substrate must be judiciously chosen.

To deal with (i) we determine the membrane phase velocity c_R from a suitable linear regression that uses as input the resonator size D, the measured frequencies, and their mode indices which can be identified from the frequency ratios between the harmonics and the fundamental mode. We find an excellent correlation that yields $c_R = 576.8\,ms^{-1}$ ($566.8\,ms^{-1}$) for the drum (square).

Our model is in excellent agreement with the observed trends providing internal dissipation (ii) is incorporated by adding to the calculated clamping loss an overall offset $1/Q_{int}$ which is left as a fit parameter. One should note that: (a) internal dissipation has been identified as a relevant mechanism in previous experiments on high-stress Si_3N_4 resonators, with indications of surface effects playing a substantial role [11, 15], and (b) our analysis does not necessarily rule out a minor frequency variation for this additional mechanism which would be masked by the non-monotonic behavior of the clamping loss (see below). To elucidate (iii) one needs to compare the wavelengths of the resonant "support" modes with the thickness of the Si wafer (0.5mm). For the square the resonant frequencies are in the MHz range resulting in wavelengths in Si (4-8mm) much larger than the wafer's thickness so that these modes are dominated by the properties of the underlying piezo and positioning system. Thus, we adopt $\nu_s = 1/3$ and leave the density ρ_s and Young modulus E_s as fit parameters. On the other hand for the drum the resonances studied lie in the $100\,MHz$ range so that the elastic wave radiation is determined mostly by the anisotropic properties of crystalline Si. For this case we adopt $\rho_s = 2.33\,gcm^{-3}$ and $\nu_s = 0.28$, but leave E_s as a fit parameter given the isotropic nature of our model.

In both cases, drum and square geometry, we find a class of modes that consistently exhibit lower dissipation $1/Q$ when compared to nearby modes [cf. Fig. 1 (c) and (d)]. Their measured Q remains approximately constant as the harmonic index is increased, leading to a growth in their fQ product that for the square reaches a maximum of 1.0×10^{13}Hz for the $(6,6)$ harmonic. These "special" classes of harmonics for the drum and square, respectively, $(n,1)|_{n>0}$ and $(n,n)|_{n>1}$ and correspond to the presence of nodal lines that intersect the periphery at evenly spaced points [cf. Fig. 1 (a) and (b)]. In contrast, for the square geometry the modes $(n,1)$, $(1,n)$, where two of the sides do not intersect any nodal lines, tend to exhibit smaller Q for comparable frequencies with $fQ \sim 10^{12}$Hz. An intuitive heuristic understanding of these trends emerges from realizing that for low harmonics, with membrane wavevectors $\sim \pi/D$, the typical resonant wavelengths in the substrate are much larger than D. Thus, for the special modes the clamping loss is suppressed [cf. Fig. 1 (e) and (f)] due to destructive interference between the waves radiated by the different equivalent segments of the periphery, defined by the nodal lines, which have alternating π-phases. Concomitantly, unlike the fundamental mode, these special modes are associ-

ated to stress sources with vanishing total force.

A quantitative grasp of these striking features can be gained by exploiting the smallness of the η_γ underpinning the aforementioned wavelength separation. For the drum, relevant harmonics satisfy the condition $\eta_\gamma \zeta_{nm} \ll \sqrt{n+1}$ which allows us to Taylor expand the Bessel functions in the $\tilde{u}_{l,\gamma}$ yielding an approximation for Eq. (2) that implies the following [26]:

$$Q_{01} \approx \left. \frac{\rho_s c_t^3}{2\pi^2 \sigma_R c_R^2 \omega_{01} \tilde{u}_0(\nu_s)} \right|_{\nu_s = 1/3} = 0.029 \sqrt{\frac{\rho_R}{\rho_s} \left(\frac{E_s}{\sigma}\right)^3} \frac{D}{\mathsf{t}}$$

$$\frac{Q_{n1}}{Q_{01}} \sim n^{\frac{2n+1}{16}} \left(0.517 \frac{c_s}{c_R}\right)^{2n}, \quad \frac{Q_{nm}}{Q_{n1}} \approx \left(\frac{\zeta_{n1}}{\zeta_{nm}}\right)^{2n+1} \quad (4)$$

where $\sigma_R = \rho_R \mathsf{t}$ is the surface mass density of the membrane and $\tilde{u}_0(\nu_s) \equiv \sum_\gamma (c_t/c_\gamma)^3 \tilde{u}_{0,\gamma}(0, \nu_s)$. Thus, the clamping-loss limited Q-values of modes $(n, 1)$ effectively grow exponentially — as the super-exponential factor plays a negligible role for relevant n, in sharp contrast to series of modes for which m is increased while n is kept constant. These exhibit a decrease of Q_{clamp} for increasing frequency [27]. On the other hand, for the square geometry analogous considerations imply for $m \sim n \gg \zeta_{01}/2\pi\eta_\gamma$ a rise in Q_{clamp} that is merely linear, with the damping rate tending to a constant value, as the harmonic indices are increased with their ratio m/n fixed. In turn, for our setting given the magnitude of $1/Q_{\text{int}}$ all the high-Q modes present roughly constant Q-values.

A comparison between the predictions [cf. Eqs. (2) and (3)] for the two geometries (with appropriate dimensions) also reveals that for "special" harmonics $[(n, 1)|_{n>0}$ and $(n, n)|_{n>1}]$ with the same frequency and number of nodal lines the circular geometry always yields a higher Q. In turn, one should note that the scalings, embodied in Eq. (4), for the Q-values in terms of ρ_R/ρ_s, E_s/σ, and D/t are completely general and independent of the shape of the boundary. These, directly imply that the fQ_{clamp} product of a given harmonic is independent of D. Furthermore, typical parameters yield for the fundamental mode $fQ_{\text{clamp}} \sim 10^{12}$Hz, which is comparable to experimental values (cf. Fig. 1 (c) and (d), and Refs. 13, 9). Finally, we have performed similar calculations for doubly-clamped beams under high-stress (nanostrings) which will be presented elsewhere. We find that though destructive interference leads to an enhancement of the Q for antisymmetric modes with low n as compared to symmetric modes, within each parity Q decreases with harmonic index so that there are no modes resilient to elastic-wave radiation as for the 2D geometries.

In conclusion, we find that the dissipation of different harmonics of a given membrane resonator exhibit a striking non-monotonic behavior which can be understood in terms of how the mode-shapes of different harmonics influence the clamping loss. We find classes of modes for which the measured Q remains approximately constant and substantially larger than for other modes with comparable frequency, and explain this phenomenon in terms of destructive interference between the radiated waves leading to a strong suppression of the clamping loss. Notably, our analysis implies that for modes $(n, 1)$ of a circular geometry, the damping rate due to elastic-wave radiation vanishes exponentially in n rendering them "asymptotically mute". Thus, for typical parameters, these azimuthal harmonics can be regarded as effectively clamping-loss free for moderate n (e.g. $fQ_{\text{clamp}} \gtrsim 10^{17}$Hz for $n \geq 5$ and thickness $\mathsf{t} < 100$ nm). Our results are relevant to state-of-the-art dispersive optomechanical setups [9, 13] and the model is also applicable to graphene nanodrums under tension [28]. Finally, we highlight that the interference effects we have unveiled will also be operational for the flexural modes of rigid plates.

---

* ignacio.wilson-rae@ph.tum.de

[1] H. G. Craighead, Science **290**, 1532 (2000); K. L. Ekinci and M. L. Roukes, Rev. Sci. Instrum. **76**, 061101 (2005).
[2] J. D. Teufel *et al.*, Nature Nanotech. **4**, 820 (2009).
[3] T. Rocheleau *et al.*, Nature **463**, 72 (2010).
[4] A. D. O'Connell *et al.*, Nature **464**, 697 (2010).
[5] A. Schliesser *et al.*, Nature Phys. **5**, 509 (2009).
[6] S. Groblacher *et al.*, Nature Phys. **5**, 485 (2009).
[7] A. D. Armour, M. P. Blencowe, and K. C. Schwab, Phys. Rev. Lett. **88**, 148301 (2002).
[8] M. Blencowe, Phys. Rep. **395**, 159 (2004).
[9] D. J. Wilson *et al.*, Phys. Rev. Lett. **103**, 207204 (2009).
[10] S. S. Verbridge *et al.*, J. Appl. Phys. **99**, 124304 (2006).
[11] S. S. Verbridge *et al.*, Nano Letters **7**, 1728 (2007).
[12] S. S. Verbridge, H. G. Craighead, and J. M. Parpia, Appl. Phys. Lett. **92**, 013112 (2008).
[13] J. D. Thompson *et al.*, Nature **452**, 72 (2008).
[14] D. R. Southworth *et al.*, Phys. Rev. Lett. **102**, 225503 (2009).
[15] Q. P. Unterreithmeier, T. Faust, and J. P. Kotthaus, Phys. Rev. Lett. **105**, 027205 (2010).
[16] M. C. Cross and R. Lifshitz, Phys. Rev. B **64**, 085324 (2001); D. S. Bindel and S. Govindjee, Int. J. Numer. Meth. Eng. **64**, 789 (2005).
[17] I. Wilson-Rae, Phys. Rev. B **77**, 245418 (2008).
[18] G. Anetsberger *et al.*, Nature Photon. **2**, 627 (2008).
[19] M. Eichenfield *et al.*, Nature **462**, 78 (2009).
[20] G. D. Cole *et al.*, (2010), arXiv:1007.4948v1.
[21] K. F. Graff, *Wave Motion in Elastic Solids* (Dover, New York, 1991).
[22] See supplementary material at. . . .
[23] The average thickness of the membrane is inferred from modelling the isotropic etching process in each material.
[24] P. Mohanty *et al.*, Phys. Rev. B **66**, 085416 (2002); C. Seoánez, F. Guinea, and A. H. Castro Neto, *ibid.* **77**, 125107 (2008); L. G. Remus, M. P. Blencowe, and Y. Tanaka, *ibid.* **80**, 174103 (2009).
[25] A. Venkatesan *et al.*, Phys. Rev. B **81**, 073410 (2010).

[26] The approximate scaling for Q_{n1}/Q_{01} differs from the results of applying Eq. (2) by at most a factor of 2 for $0 < n < 15$ in the relevant regime $\eta_t < 0.3$ and $\nu = 1/3$.

[27] For such modes, $\eta_\gamma \zeta_{nm} \ll \sqrt{n+1}$ eventually fails and for $\eta_\gamma \zeta_{nm} \gg n^2$ one finds that $1/Q_{nm}$ is oscillatory.

[28] C. Chen *et al.*, Nature Nanotech. **4**, 861 (2009).